5

The Corona Discharge

M. KHALIFA *Cairo University, Giza, Egypt*

M. ABDEL-SALAM *Assiut University, Assiut, Egypt*

5.1 INTRODUCTION

"Corona" literally means the disk of light that appears around the sun. The term was borrowed by physicists and electrical engineers to describe generally the partial discharges that develop in zones of highly concentrated electric fields, such as at the surface of a pointed or cylindrical electrode opposite to and at some distance from another. This partial breakdown of air is quite distinct in nature and appearance from the complete breakdown of air gaps between electrodes. The same applies for other gases.

The corona is also distinct from the discharges that take place inside gas bubbles within solid and liquid insulation, although the underlying phenomena of gas discharges are the same. The corona discharge is accompanied by a number of observable effects, such as visible light, audible noise, electric current, energy loss, radio interference, mechanical vibrations, and chemical reactions. The chemical reactions that accompany corona in air produce the smell of ozone and nitrogen oxides.

Corona has long been a main concern for power transmission engineers because of the power loss it causes on the lines and the noise it causes in radio and TV reception. On the other hand, corona does have several beneficial applications, as in Van de Graaff generators, electrostatic preci-

pitators, electrostatic printing, electrostatic deposition, ozone production, and ionization counting (Berg and Hauffe, 1972; Landham et al., 1987; Seelentag, 1979), as described in detail in Chapter 19.

5.2 MECHANISM OF CORONA DISCHARGE

The discharge process depends on the polarity of the applied voltage. Therefore, it will be discussed first for each polarity under DC.

5.2.1 Positive Corona

At the onset level, and slightly above, there exists a small volume of space at the anode where the field strength is high enough to cause ionization by collision. When a free electron is driven by the field toward the anode, it produces an electron avalanche (Chapter 3). The cloud of positive ions produced at the avalanche head near the anode forms an eventual extension to the anode. Secondary generations of avalanches get directed to the anode and to these dense clouds of positive ions (Fig. 5.1). This mode of corona consists of what are called onset streamers. If conditions are favorable, the high field space at the anode may suit the formation of streamers extending tangentially onto the anode; these are called "burst-pulse streamers" (Loeb, 1965).

At slightly higher voltages a cloud of negative ions may form (Fig. 5.1) near the anode surface such that the onset-type streamers become very numerous. They are short in length, overlap in space and time, and the discharge takes the form of a "glow" covering a significant part of the HV conductor surface (Fig. 5.2b). The corresponding current through the HV circuit becomes a quasi-steady current (Fig. 5.2). This is in contrast with current pulses corresponding to onset streamers (Fig. 5.2) (Giao and Jordan, 1967; Khalifa, 1979). The positive current pulse corresponds to a succession of generations of electron avalanches taking place in the ionization zone at the anode (Khalifa and Abdel-Salam, 1974a).

At still higher voltages the clouds of negative ions at the anode can no longer maintain their stability and become ruptured by violent pre-breakdown streamers, corresponding to irregular, high-amplitude current pulses (Figs. 5.1 and 5.2). If we continue to raise the voltage, breakdown eventually occurs across the air gap. Figure 5.3 presents the range for each type of corona discharge with positive DC voltage applied across a point-to-plane gap (Nasser, 1971).

5.2.2 Negative Corona

At the onset level and slightly higher, the corona at the cathode has a rapidly and steadily pulsating mode; this is known as Trichel pulse corona. Each

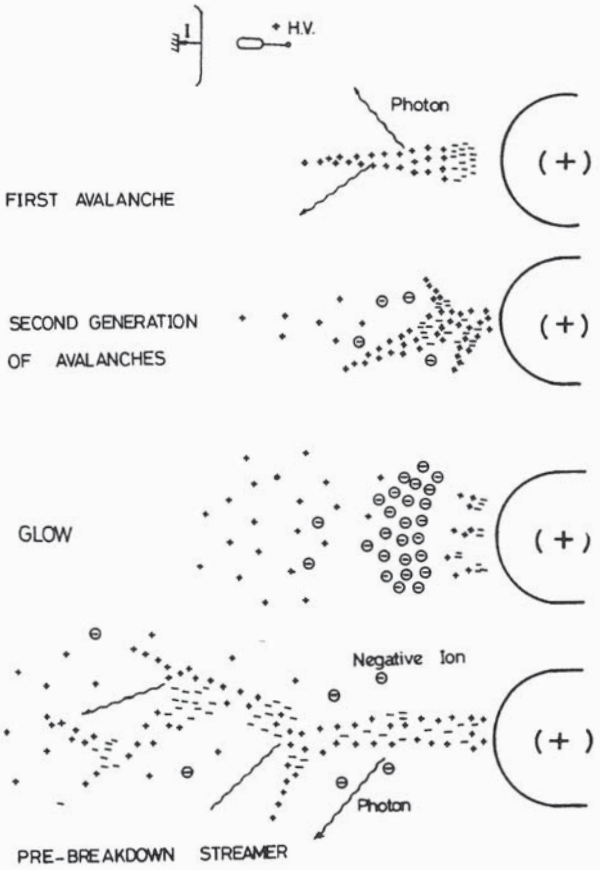

Figure 5.1 Development of the first and subsequent generations of avalanches in positive corona discharges.

current pulse corresponds to one main electron avalanche occurring in the ionization zone (Fig. 5.4) (Khalifa and Abdel-Salam, 1974b; Zeitoun et al., 1976). In this case the ionization zone extends from the cathode surface outward and as far as the point where the field becomes too weak for ionization by collision to compensate for electron attachment. Beyond such a point, more and more of the avalanche electrons get attached to gas molecules and form negative ions which continue to drift very slowly away from the cathode. During the process of avalanche growth, some photons radiate from the avalanche core in all directions (Fig. 5.4). The photoelectrons thus produced can start subsidiary avalanches that are directed from the cathode. The motion of the electrons and negative ions away

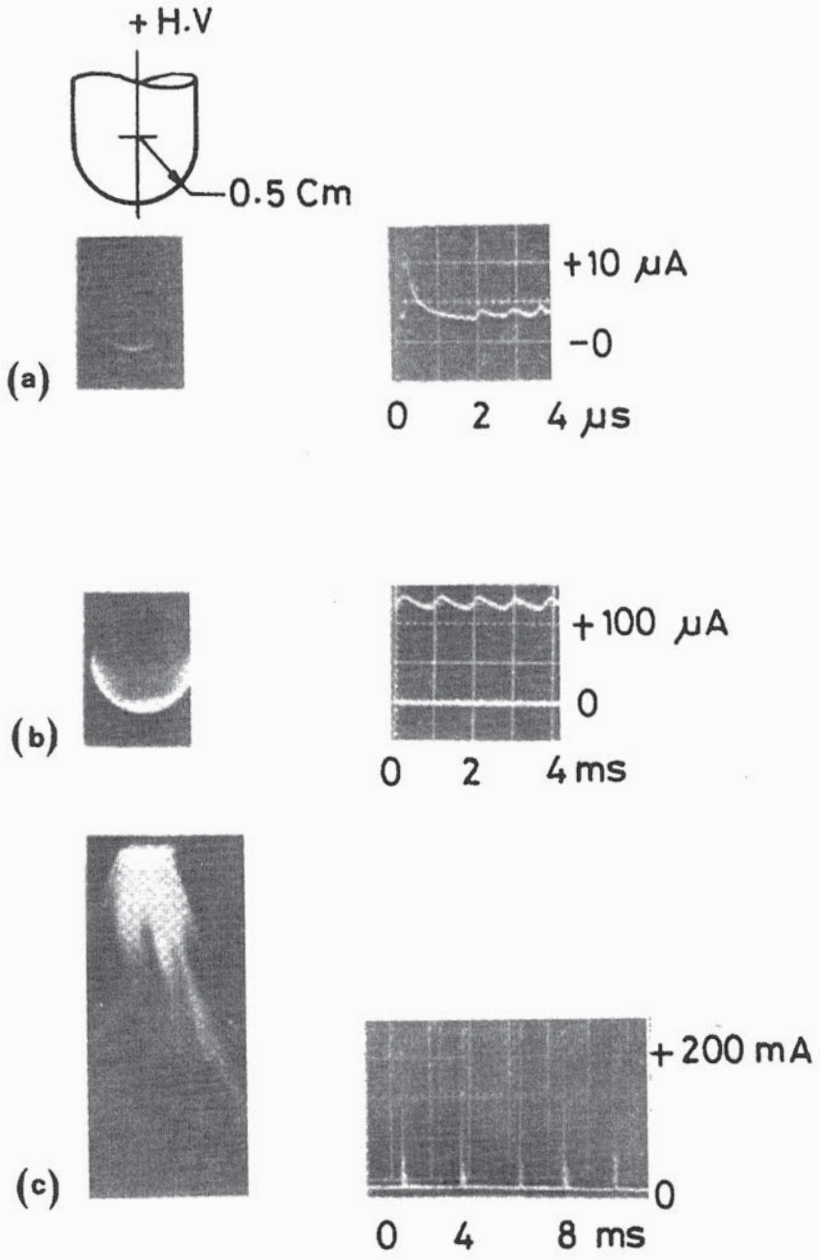

Figure 5.2 Photographs and corresponding current oscillograms of different modes of positive corona. [From Giao and Jordan (1967).]

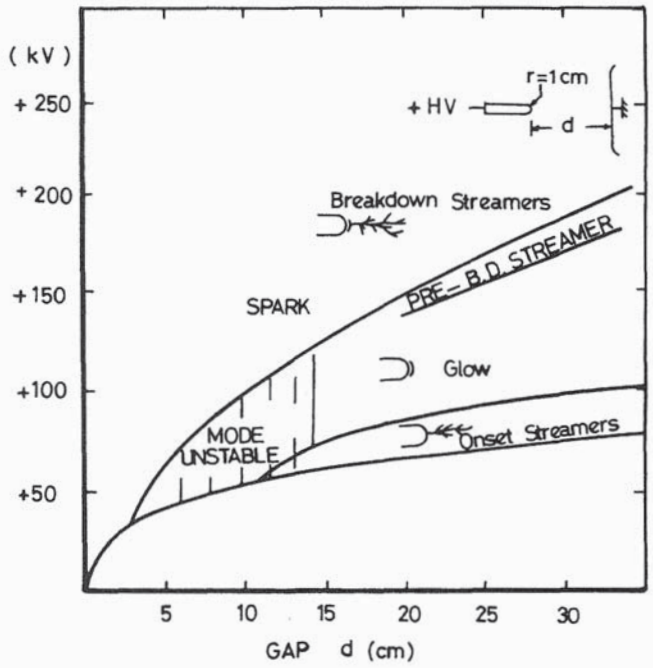

Figure 5.3 Onset voltages of various positive corona modes and sparkover voltage as functions of point-to-plane gap spacing. [Courtesy of E. Nasser (1971) and Wiley-Interscience.]

from the cathode and that of positive ions toward it correspond to the corona current pulses flowing through the high-voltage circuit, as shown in Figure 5.5a, and can easily be computed.

With an increase in applied voltage, the Trichel pulses increase in a repetitive rate up to a critical level at which the negative corona gets into the steady "negative glow" mode (Figs. 5.4 and 5.5b). At still higher voltages pre-breakdown streamers appear, eventually causing a complete breakdown of the gap (Figs. 5.4 and 5.5c).

5.2.3 AC Corona

The basic difference between AC and DC coronas is the periodic change in direction of the applied field under AC, and its influence on the residual space charge left over from the discharge during preceding half-cycles (Fig. 5.6). Thus positive onset streamers and burst-pulse streamers may appear only over an extremely small range of voltage at onset, followed by a posi-

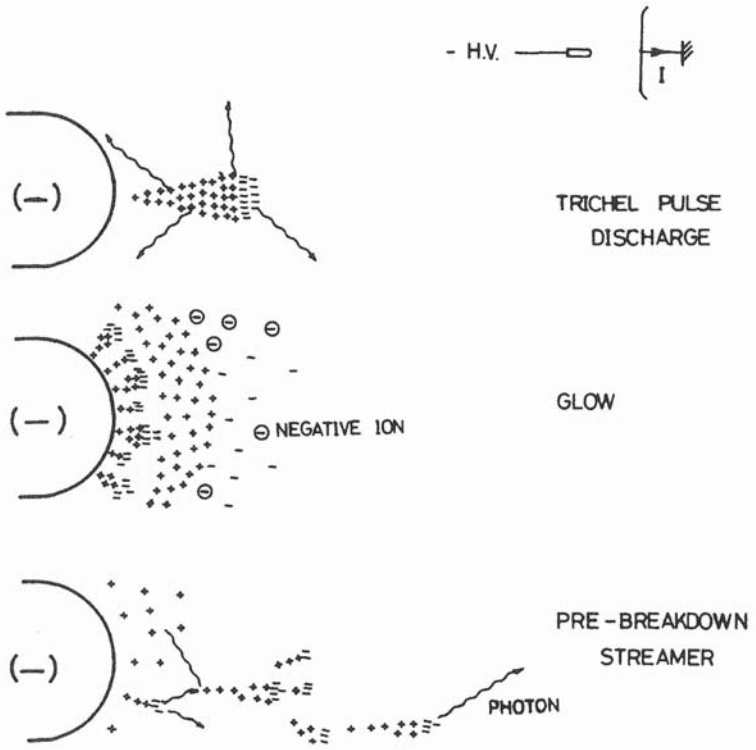

Figure 5.4 Development of electron avalanches in negative corona discharges.

tive glow. Both negative Trichel pulses and negative glow can be observed in an AC corona. If the applied voltage has a suitable magnitude, then, depending on the electrode geometry, both positive and negative glows and streamer coronas can be observed in each cycle.

5.2.4 Impulse Corona

Under impulse voltages, the corona starts in an air gap almost clear of any space charge. Therefore, electron avalanches and streamers extend over significant distances. The onset streamers produced and their branches can easily form traces on photographic films in contact with the anode or cathode, in what is known as Lichtenberg figures (Fig. 5.7). Such a figure cannot be produced by DC because of the choking effect of accumulating clouds of space charges. Under AC a very large number of traces get superimposed on each other.

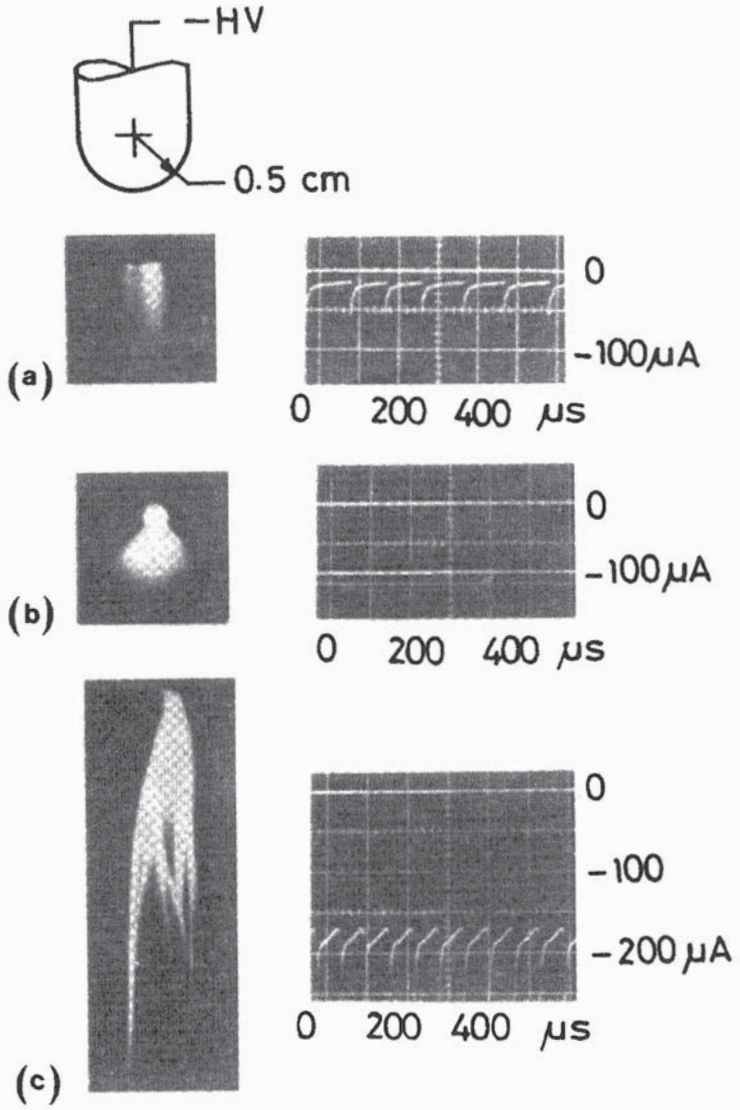

Figure 5.5 Photographs and corresponding current oscillograms of various modes of negative corona. [From Giao and Jordan (1967).]

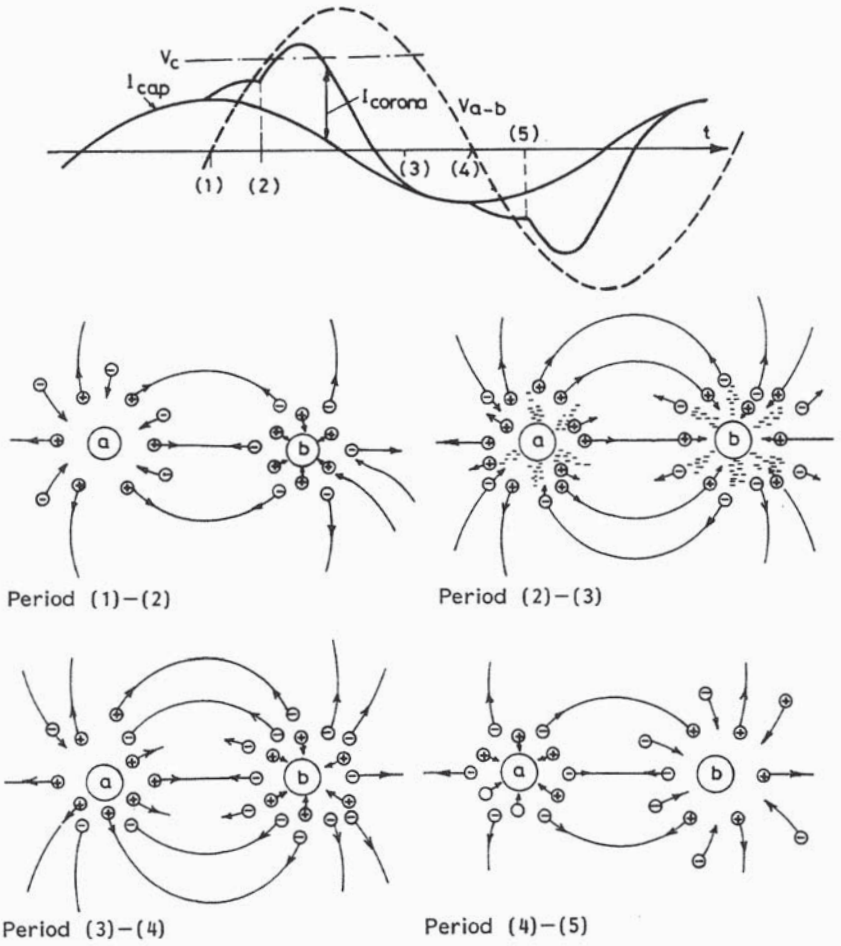

Figure 5.6 AC corona current for a symmetrical gap between two parallel conductors a and b. Note that when the voltage V_{a-b} is below the corona-onset level V_c, the corona current corresponds to the motion and recombination of residual ions in the gap between the high-voltage conductors during the periods shown in the oscillogram.

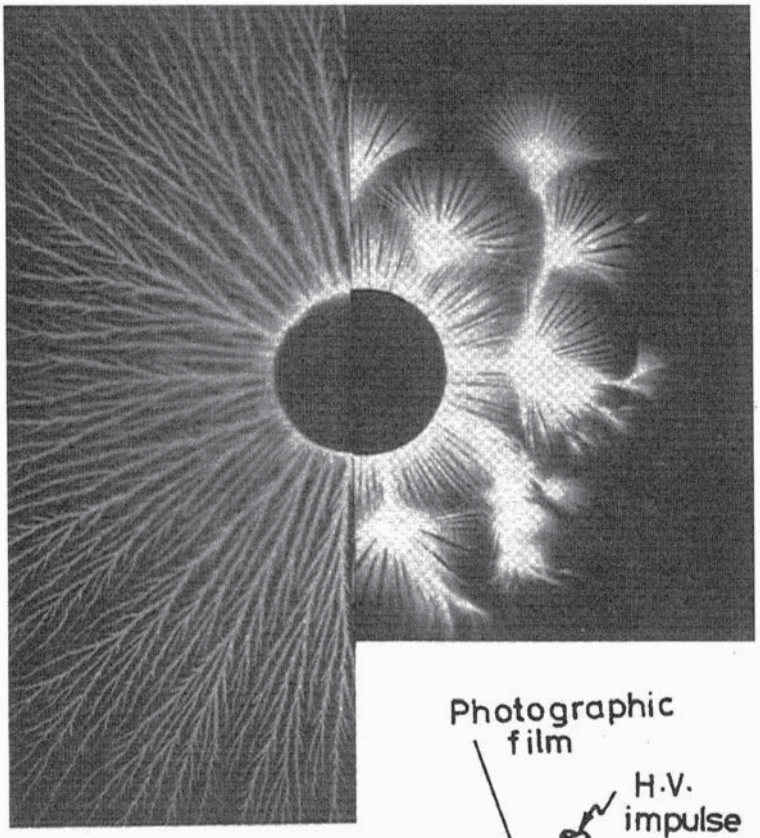

(a)

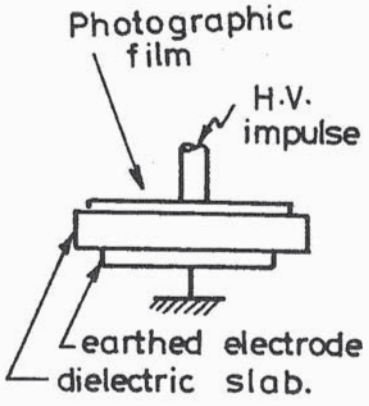

(b)

Figure 5.7(a) Photographic traces of corona discharge under impulse voltage (Lichtenberg figures): (left) positive polarity; (right) negative polarity; (b) test setup.

On long HV transmission lines, the current corresponding to corona discharges under traveling extra-high-voltage surges has the beneficial effect of reducing the surge peak and front steepness, as shown by experiment and computation (Chapter 14). Thus their stresses on the power system insulation are relieved.

5.3 THE CORONA ONSET LEVEL

It has been well established by experiment and by computation that corona discharge starts at the surfaces of HV electrodes and conductors when their surface voltage gradients reach a critical value E_0 (Abdel-Salam and Khalifa, 1977). The magnitude of E_0 depends on the voltage polarity and on the pressure and temperature of the ambient gas. Humidity has a minor effect. The air pressure p (kPa) and temperature θ (°C) are usually combined into one factor δ, the relative air density, referred to STP. Thus

$$\delta = \frac{2.94p}{273 + \theta} \tag{5.1}$$

with δ ranging between 0.9 and 1.1. Experimentally measured E_0 values fit the following relations:

For AC:

$$E_0 = 30\delta \text{ kV}_{\text{peak}}/\text{cm} \tag{5.2}$$

For DC:

$$E_{\pm} = A_{\pm}\delta + B_{\pm}\sqrt{\frac{\delta}{r}} \text{ kV/cm} \tag{5.3}$$

A_+ and A_- are in the respective ranges 31 to 39.8 and 29.4 to 40.3; B_+ and B_- are, correspondingly, 11.8 to 8.4 and 9.9 to 7.3.

Under AC, a slightly higher field strength E_v corresponds to corona being clearly visible on the conductor surface and can be expressed as $E_v = 30\delta(1 + 0.3/\sqrt{\delta r})$ $\text{kV}_{\text{peak}}/\text{cm}$, r being the conductor radius in centimeters.

5.3.1 The Corona Onset Voltage

This can easily be calculated using E_0 or $E_{\pm}$ once the conductor arrangement and dimensions are known. Methods of field calculations were discussed in Chapter 2. It should be realized that field calculations would normally be based on the assumption of perfectly clean, smooth conductors; this is different from practical conditions. At any point of microroughness on a practical conductor surface the field will be highly concentrated and the

critical field strength for corona onset will be reached there, while the average field strength over the entire surface remains considerably lower. A corresponding surface factor should be taken into account while estimating the corona onset voltage V_0 for the conductor arrangement. This factor is usually taken as about 0.6 for new rough-stranded conductors and about 0.85 for weathered conductors.

5.3.2 Computation of DC Corona Onset Voltages

Onset voltages of DC corona can be estimated using the relation (5.3). They can also be computed according to an algorithm based on the ionization and deionization process acting in a corona discharge of either polarity (Khalifa and Abdel-Salam, 1974a).

5.3.2.1 Case of Positive Polarity

The first avalanche proceeds toward the anode and ends at its surface. It develops a cloud of positive ions, and photons are emitted from its core. Due to the photo-ionization process, these photons generate photoelectrons to start successor avalanches (Fig. 5.8). At corona onset voltage, the number of electrons N_1 in the first avalanche is equal to the number N_2 in the

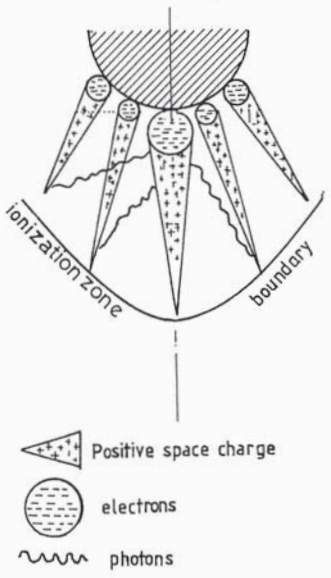

Figure 5.8 Development of the primary avalanche and its successors in the vicinity of a positive stressed electrode.

successor avalanches, and the first avalanche becomes unstable. This instability results in the formation of luminous filamentary streamers (Loeb, 1965; Nasser, 1971). Therefore, it is implied that the level of ionization in the successor avalanches is such that sufficient photons and hence photoelectrons will be generated to make the ionization self-sustained when

$$N_2 \geq N_1 \tag{5.4}$$

The onset voltage does not appear explicitly in the relation (5.4), and the onset voltage is the critical value which fulfills the equality (5.4) (Khalifa and Abdel-Salam, 1974a). The computed onset voltages are in good agreement with experiment (Abdel-Salam, 1985).

5.3.2.2 Case of Negative Polarity

When the applied electric field strength near the cathode surface reaches the threshold value for ionization of gas molecules by electron collision, an electron avalanche starts to develop along the direction away from the cathode (Fig. 5.9). With the growth of the avalanche, more electrons are developed at its head, more photons are emitted in all directions, and more positive ions are left in the avalanche wake.

For a successor avalanche to be started, the preceding avalanche should somehow provide an initiating electron at the cathode surface, pos-

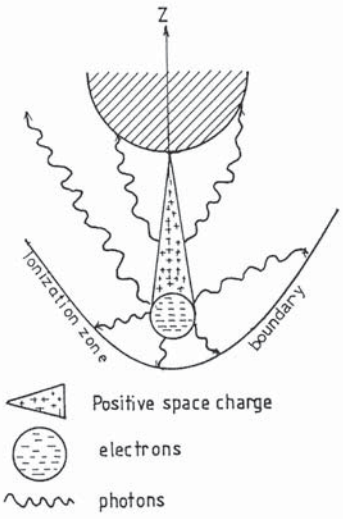

Figure 5.9 Development of an avalanche in the vicinity of a negative stressed electrode.

sibly by photoemission, positive ion impact, metastable action, or field emission. Field emission is possible only at field strengths exceeding 5×10^7 V/m (Rein et al., 1977). Electron emission by positive ion impact is more than two orders of magnitude less probable than photoemission (Loeb, 1965). Metastables have been reported to have an effect approximately equal to that of positive ion impact (Nasser, 1971). Therefore, only the first mechanism (electron emission from the cathode by photons) was considered in the mathematical formulation of the onset criterion, where at least one photoelectron is emitted by the photons of the first avalanche to keep the discharge self-sustaining, i.e.,

$$N_{e\,ph} \geq 1 \tag{5.5}$$

where $N_{e\,ph}$ is the number of electrons photoemitted from the cathode.

The onset voltage does not appear explicitly in the relation (5.5), and the onset voltage is the critical value which fulfills the equality (5.5) (Khalifa and Abdel-Salam, 1974a). The computed onset voltages are in good agreement with experiment (Khalifa and Abdel-Salam, 1974b; Abdel-Salam and Stanek, 1988).

It is known that the onset voltage gradient for a positive corona is slightly lower than that for a negative corona. Therefore, the voltage level corresponding to positive corona onset can be calculated according to the method described above for a monopolar corona. At the negative conductor, which has not yet reached its corona onset level, there are positive ions drifting toward it and coming from the positive corona discharge at the positive conductor. These ions enhance the field intensity at the negative conductor and cause a corona to start at a voltage slightly lower than the value calculated for the monopolar case. This slight difference can also be computed (Abdel-Salam and Khalifa, 1977; Al-Hamouz et al., 1998).

5.3.3 Computation of DC Corona Pulse Characteristics

5.3.3.1 Case of Positive Polarity

Positive pulsating corona discharges occur near the onset level as onset streamers and at much higher voltages as pre-breakdown streamers (Nasser, 1971). The streamer is built up by a number of successive generations of electron avalanches which take place in the ionization zone around the positive HV electrode (Khalifa and Abdel-Salam, 1974b).

The ionization zone around the HV electrode is defined as the space where the resultant field strength is so high that the first Townsend's coefficient of ionization is greater than the coefficient of electron attachment. With successions of avalanches and accumulation of ion space charges, the ionization zone expands and its contour changes.

The electrons are driven to the electrode by the resultant of the field of the applied voltage and the field of the space charge. They become involved with air molecules in exciting and ionization collisions to produce an avalanche. Photons are emitted by the avalanche in various directions. Photoelectrons are produced in various locations from which they start a new generation of avalanches. Each photoelectron produced within the ionization zone will be accelerated by the prevailing field from its point of origin and start one avalanche of the second generation. Most of the new avalanches of the succeeding generation get started almost at the instant of termination of the previous avalanche when its population of electrons is highest.

The corona current through the HV circuit corresponds to the motion of electrons and ions in the space between the HV conductors. The motion of ions can be safely neglected as compared to that of electrons during the corona pulse. Thus, the instantaneous current of a given generation of avalanches is calculated as the sum of the components corresponding to the individual avalanches.

In experiment, the capacitance of the HV and measuring circuits smooths the variation of the current from instant to instant during the life of each generation, which is of the order 1 ns, and the current is averaged over the life of each generation. The calculations are continued over successive generations until the magnitude of the current falls below 1% of the maximum value reached for any generation. The current pulse is then considered to have ended.

5.3.3.2 Case of Negative Polarity

Different from the positive case, the negative corona pulse corresponds to one primary avalanche accompanied by a series of auxiliary avalanches which develop in the discharge zone around the HV electrode during the life of the primary avalanche (Khalifa and Abdel-Salam, 1974b).

The primary avalanche is initiated by an electron driven by the electric field outwards from a point of microroughness on the conductor surface. By ionizing and exciting collisions with the air molecules, more and more electrons, photons, and a cloud of positive ions are produced in the primary avalanche.

The photons reaching the conductor emit new electrons of number N_p which start the successor avalanches. When N_p reaches unity (i.e., when the first electron leaves the conductor) the first successor avalanche gets launched. It grows in the same way as the primary avalanche and contributes to the irradiation of the conductor surface, leading to the emission of more and more photoelectrons which start new successor avalanches, and so on.

As the electrons drift away from the conductor in the decreasing field, more and more of them get attached to air molecules and form negative ions. The positive and negative ion clouds grow with time as more avalanches are formed. The space where the field strength is high shrinks and eventually no more avalanches can develop.

The magnitude of the corona pulse current at any instant is calculated as the sum of the current components corresponding to the individual avalanches.

The shapes and durations of the calculated positive and negative pulses agree quite closely with experiment. Different from positive pulses, the calculated negative pulse amplitudes are almost equal to those measured (Khalifa and Abdel-Salam, 1974b).

5.3.3.3 Pulse Amplitudes and Repetition Rates

The amplitudes of the positive and negative corona pulse are evaluated during the process of calculations as the maximum values obtained in the computations of the current pulse. Also, charge contents of the pulses are easily evaluated by integrating the current waves. To calculate the pulse repetition rates, one has to define the conditions to be fulfilled after the termination of a pulse in order that the subsequent pulse can be initiated (Khalifa and Abdel-Salam, 1974b).

In the case of a positive pulse, the favorable condition is taken as the positive ion clouds being swept so far from the high-voltage electrode that their residual field at the boundary of the ionization zone becomes negligible, i.e., 0.1% of the field strength produced there by the applied voltage.

For negative pulses, the new pulse will not start until both positive and negative ion space charges have left the discharge zone. The positive ions are swept to the HV electrode, where they are neutralized. The negative ions move so far from the electrode that their residual field strength at the boundary of the discharge zone becomes negligible, i.e., 0.1% of the applied field strength. The discharge-zone boundary is defined as the place where 99.9% of the electrons in the avalanches have become attached to air molecules and formed negative ions. The calculated pulse repetition rates are closer to those measured. The bigger the charge content of the calculated pulses, the longer the time they take to disappear from the ionization zone and allow for the initiation of the next pulse, and the smaller the repetition rate (Khalifa and Abdel-Salam, 1974b).

5.3.4 Possible Corona in Compressed Air and SF_6

Because sulfur hexafluoride is an electronegative gas, it has a high affinity for electron attachment. This makes it more difficult for electron avalanches

to grow. Thus corona and sparkover occur at voltages considerably higher than those in air. Above a certain critical gas pressure sparkover occurs across the gas gap without any preceding corona (Section 4.4). At such high pressures the coefficient of ionization by collision becomes lower than the coefficient of electron attachment: $\alpha < \eta$ (Chapter 3). Thus electrons produced at the cathode by photoemission and field emission would have to contribute more substantially to the discharge in order to maintain its stability. Taking both these processes into account has made possible the computation of breakdown voltages of gaps in compressed air and SF_6 (Khalifa et al., 1977; Abdel-Salam, 1978).

5.4 CORONA POWER LOSS

5.4.1 Corona Loss Formulas

Empirical formulas have been suggested for evaluating corona losses on AC lines and on both monopolar and bipolar DC lines.

5.4.1.1 AC Lines

Empirical formulas were suggested early in this century by Peek and Peterson for estimating P_c, the fair-weather corona losses of overhead transmission lines (Begamudre, 1986). Because of several flaws, Peek's formula was superseded by that of Peterson, which takes the form

$$P_c = \frac{3.73K}{(D/r)^2} fV^2 \times 10^{-5} \text{ kW/conductor} \cdot \text{km} \tag{5.6}$$

where f is the frequency, V the line voltage, and D and r the phase conductor separation and radius. K is a factor depending on the ratio of the operating voltage V to the corona onset line voltage V_0 (Fig. 5.10).

A much more recent and more scientific approach was the computer program developed by Abdel-Salam et al. (1984) on the basis of the physical phenomena of corona discharge (Shamloul, 1989).

In properly designed transmission lines, the corona loss in fair weather is usually insignificant. Typical values measured range from 0.3 to 1.7 kW/conductor·km for 500 kV lines and from 0.7 to 17 kW/conductor·km for 700 kV lines (Electrical Power Research Institute, 1979).

Effect of Conductor Bundling. For transmission lines with bundled conductors, Peterson's formula can be modified by including the capacitance geometric mean radius of the bundle instead of the single-conductor radius. Naturally, the separation between subconductors in the bundle has an effect on the amount of corona loss. There is an optimal separation between subconductors in the bundle that corresponds to minimum corona loss.

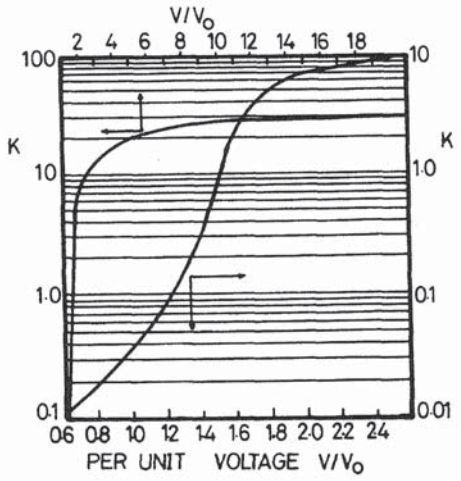

Figure 5.10 Factor K to be used in Peterson's corona loss formula as a function of the per-unit operating voltage referred to the corona-onset voltage.

Effects of Weather. The principal weather parameters are air temperature, pressure, wind, humidity, rain, snow, and dust. The air temperature and pressure are included in the factor δ. No perceptible effect of wind on the AC corona can be noticed. The same goes for humidity unless it approaches 100%. With condensation, and much more seriously with rain, the corona losses increase 10-fold or more, depending on the rate of rainfall (Electrical Power Research Institute, 1979). The increase in corona loss due to rain and dust on conductors of large diameter is much greater than with smaller conductors, as the coronating points are more numerous in the former case.

5.4.1.2 DC Lines

In unipolar DC lines, we have ions of only one polarity in the space between conductors, and between the conductors and ground. With bipolar lines, however, we have both positive and negative ions in the interconductor space and there is a high probability of ion recombination. This particular phenomenon accounts for the corona loss on bipolar DC lines being much higher than on monopolar lines, and even higher than on AC lines, as computed by Abdel-Salam et al. (1982).

In comparison with AC lines having equal per-unit effective voltages with respect to the corona onset levels, the fair-weather corona loss on a bipolar line was found to be about twice that on a three-phase AC line. On

the other hand, increases in bipolar line corona loss with voltage and in foul weather are not as rapid as in the case of AC lines.

The effects of atmospheric humidity and wind can be measured and computed (Khalifa and Abdel-Salam, 1974b). The corona loss of monopolar lines can increase by about 20% if humidity increases from 60% to approaching 100%. A much more significant increase occurs if wind blows across the conductors of bipolar lines (Fig. 5.11).

5.4.2 Computation of Corona Power Loss

5.4.2.1 AC Lines

As the AC voltage applied to a single conductor reaches a critical value $V_{0\pm}$, the electric field at the conductor surface reaches the corona onset value $E_{0\pm}$. Corona starts when the electric field exceeds the onset value, and charges of the same sign as that of the conductor potential are emitted into space and move away from the conductor in the form of shells. The charge in a given shell raises the field in the space outside the shell, thus absorbing a part of the applied voltage, while reducing the field at the coronating conductor surface by provoking an increase of the induced opposite charge there (Clade et al., 1969; Abdel-Salam et al., 1984). Therefore, the emission is regulated in such a way that any increase in the space charge due to a new emission causes a reduction of the surface field and therefore a slowing down of emission. It has been realized by experiment (Waters et al., 1972) and theory (Khalifa and Abdel-Salam, 1973) that the electric field at the

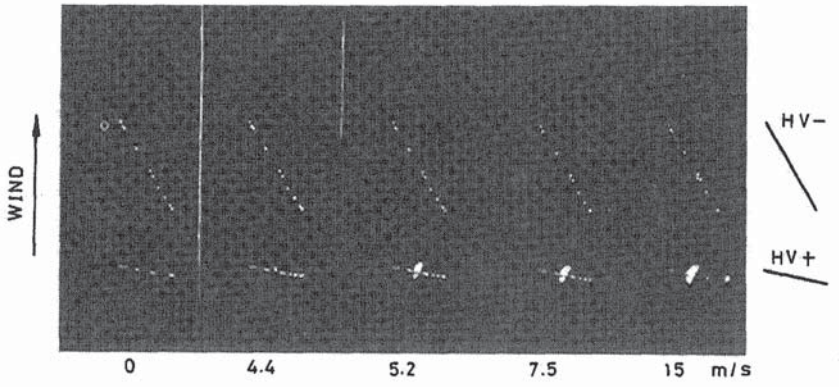

Figure 5.11 Appearance of bipolar DC corona on two conductors, 6.5 mm in diameter and 45 mm apart, at ±63 kV and at different wind speeds. The conductor arrangement is indicated.

surface of a coronating conductor assumes a value less than the onset value.

The voltage $V_{0\pm}$ is the onset voltage at which corona starts in the first positive or negative half-cycle. In the succeeding half-cycle, corona starts at voltages $V_{i\pm} < V_{0\pm}$ due to the effect of the residual space charge. $V_{i\pm}$ are termed the ionization onset voltages. It has been assumed (Clade et al., 1969) that the ionization during each cycle terminates at the voltage peak (V_p) and starts at voltage $V_{i\pm}$, determined by a simple relation

$$V_p - V_{0\pm} = V_{0\pm} - V_{i\pm} \tag{5.7}$$

Of course, $V_{i\pm} = V_{0\pm}$ for the first positive or negative half-cycles. Experiment showed that the corona terminates after the voltage peak of the positive and negative half-cycles at $V_{e\pm}$.

Many experiments have been done to study the performance of AC corona. The $V - Q$ relation is the most important outcome of these experiments to evaluate the AC corona loss (Abdel-Salam and Shamloul, 1992). The corona starting and ending voltages are prerequisites for drawing the $V - Q$ curve, whose area expresses the corona loss per cycle.

Single-phase Transmission Lines. Consider a single-phase conductor-to-plane arrangement as shown in Figure 5.12a. The conductor is simulated by a set of unknown line charges uniformly distributed inside the conductor and coaxial. The magnitudes of these line charges are determined to satisfy the boundary conditions (the potential calculated at the conductor surface

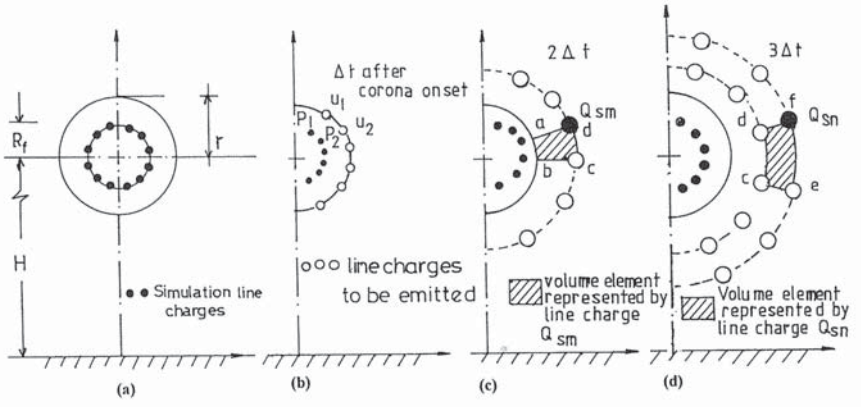

Figure 5.12 Charge development during the first half-cycle: r = conductor radius, R_f = radius of a fictitious cylinder where the simulation charges are located, and H = conductor height above ground plane.

must equal the applied voltage) at a number of boundary points equal to the number of unknowns.

When the applied voltage reaches the positive onset value V_{0+} for the first time, the magnitudes of the unknown charges, denoted as the positive onset values, are $Q_{0j+}, j = 1, 2, \ldots$.

When the applied voltage exceeds V_{0+}, ion emission starts from the conductor. The magnitudes of the unknown charges are $Q_{j+}, j = 1, 2, \ldots$.

On the assumption of constant conductor surface charge, the magnitudes of the emitted space charge Q_{sj+} are assumed (Abdel-Salam and Shamloul, 1992) to be equal to the difference between the line charges Q_{j+} and the corresponding onset values Q_{0j+}.

It is quite reasonable to model the ion emission from the wire in a discrete form; each time interval the conductor generates an infinitely thin cylindrical shell of charges. Each shell was treated (Clade et al., 1969) as a block moving away from the wire or returning back to it. Due to the presence of the ground plane, the space line charges simulating the shell are not concentric with the conductor. Even the charges $Q_{j+}, j = 1, 2, \ldots$, are determined at the points $P_1, P_2, \ldots$ (Fig. 5.12b). They start their journey at the points $u_1, u_2, \ldots$ on the conductor surface under the prevailing field (Fig. 5.12c).

The ion emission, being assumed discrete, dictates that each space line charge represents the charge over a volume element per unit length of the wire. Figures 5.12c and d show the volume elements abcd and dcef represented by the mth line charge and the nth line charge of the first and second emission respectively. The size of the volume element changes from time to time as the line charge departs away from or returns back to the conductor.

For the first negative half-cycle, ion emission starts at V_{i-} and terminates at V_{e-}, the same as explained before for the first positive half-cycle. The liberated negative space charges move away from the stressed conductor. At the same time, the positive space charge returns to the conductor and meets the outgoing negative ones. Some of the positive ions are neutralized through recombination. The space line charges continue to move in opposite directions and will undergo further recombination processes once they meet the opposite charges. Sometimes, some line charges disappear totally due to many successive recombination processes.

All the procedures described above for emission during the first cycle are repeated for the succeeding cycles until a steady-state ion emission is achieved. Corona loss depends on both the amount of charges liberated in space and displacement of these charges through the prevailing field E_f in the wire neighborhood.

The energy dissipation through a complete cycle is calculated as

$$W = \sum_{A} \int_{C} Q_{si} E_f \mathrm{d}r \tag{5.8}$$

where the summation range A is over all positive and negative space line charges Q_{si}, and C the line-charge trajectory (since its emission from the conductor surface) over a cycle. The corona power loss is simply the energy dissipation W per cycle times the frequency of the applied voltage.

The calculated corona power-loss values agreed with those measured experimentally (Abdel-Salam and Shamloul, 1992).

Three-phase Transmission Line. The proposed method of calculating the corona power loss on three-phase transmission lines is similar to that for single-phase lines. Based on the conductor radius, the positive and negative onset field values are defined for each phase conductor. Each phase conductor of the three-phase transmission line is simulated by a set of infinite line charges. The onset charge for each phase conductor will be the summation of those simulation charges located inside it (Abdel-Salam and Shamloul, 1994; Abdel-Salam and Abdel-Aziz, 1994b).

The charges simulating each phase conductor surface charge are obtained by setting the potential at each boundary point equal to the respective phase voltage. This results in a system of simultaneous linear algebraic equations whose solution evaluates the simulation line charges of each phase. The emission law is similar to that in the single-phase case in which, whenever the magnitude of the conductor charge of any phase exceeds the onset value, the surplus charge is emitted as space line charges. Space line charges are displaced under the electric field due to the conductor as well as the space line charges for the three phases. Also, recombination between positive and negative space line charges is taken into account. Corona energy loss is calculated by

$$W = \sum_{3\text{phases}} \sum_{A} \int_{C} Q_{si} E_f \mathrm{d}r \tag{5.9}$$

Corona power loss is calculated by multiplying the corona energy loss by the system frequency. The calculated values of corona power loss agreed satisfactorily with those measured (Abdel-Salam and Shamloul, 1994; Abdel-Salam and Abdel-Aziz, 1994b). More detailed calculations of three- and six-phase corona power loss are reported elsewhere (Abdel-Salam and Abdel-Aziz, 2000).

5.4.2.2 DC Lines

The corona power loss on monopolar and bipolar DC lines was computed using finite-element and charge-simulation techniques. However, the com-

putation of corona power loss on AC lines was limited to the charge-simulation technique.

(a) Using the Charge-simulation Technique. At voltages below the onset value, the field in the inter-electrode spacing is Laplacian. At voltages above the onset value, ions are produced, forming a drifting space charge of the same polarity as that of the coronating electrode. The ions flow towards the other electrode, filling the inter-electrode spacing, where the field is Poissonian. In symmetrical arrangements, such as parallel plates or coaxial cylinders, the ions move along the Laplacian flux lines, which means that the Laplacian and Poissonian fields have the same direction. In asymmetrical arrangements, such as transmission-line arrangements, the space charge causes a deviation between the two patterns, depending on the spatial distribution of ions in the inter-electrode spacing. Thus, Deutsche's assumption, stated in Section 2.6 is no longer valid.

For the Poissonian field around DC lines, the space charge is simulated by a set of fictitious discrete charges, the same as the surface charges on the conductors as described in Section 2.4.3 (Horenstein, 1984; Elmoursi and Castle, 1986; Abdel-Salam and Abdel-Sattar, 1989; Elmoursi and Speck, 1990; Abdel-Salam and Abdel-Aziz, 1994). However, the locations of the simulation charges are located in the space outside the coronating conductor(s) where the field is to be calculated. Therefore, the locations of the simulation charges are singularity points in evaluating the potential and the electric field there. An attempt was made to evaluate the potential and field at the singularity points in a parallel-plate arrangement (Abdel-Salam and Abdel-Aziz, 1992).

As described in Section 2.6.3, the two sets of discrete charges have to be chosen to satisfy the boundary conditions of Poisson's equation (2.58). Images of these charges with respect to the ground plane are considered.

To accommodate the boundary conditions, boundary points are chosen on the coronating conductors.

Satisfaction of the boundary conditions at the boundary points results in a system of nonlinear equations whose solution determines the unknown simulation charges. The technique to solve these nonlinear equations is iterative in nature, where the solution is initialized and the electric field is updated until a self-consistent solution of the electric field and the space line charges is obtained.

The volume charge density is calculated by dividing each discrete line charge by the volume it occupies, and the current density is calculated using equation (2.58). The corona current is obtained by integrating the current density over the periphery of the coronating conductor. Multiplying the corona current by the applied voltage determines the corona power loss.

The calculated corona currents agreed with those measured on lines with single conductors (Abdel-Salam and Abdel-Aziz, 1994a) and on lines with bundled conductors (Abdel-Salam and Mufti, 1998).

(b) Using the Finite-element Technique. The first step in the finite-element formulation of Poisson's equation is to divide the area of interest (around transmission-line conductors) into triangular elements forming a grid (Aboelsaad et al., 1989; Abdel-Salam and Al-Hamouz, 1992). Poisson's equation is then transformed into a set of linear equations by minimizing the energy functional expressed by equation (2.35) over an element. Summing up for all the elements of the grid results in a set of simultaneous equations whose solution determines the unknown potentials at the nodes. The electric field can be determined; see equation (2.58).

However, determination of the electric field in the presence of space charge must satisfy the continuity of the current density, equation (2.58). Therefore, the ionized field is divided into flux (stream) tubes. Two field lines define a flux tube as field lines never cross. The continuity equation can therefore be extended to all the flux tubes.

The finite-element formulation of Poisson's equation and the continuity equation of current density are solved iteratively for the electric potential and the space charge-density. As the space-charge density is known at the coronating-conductor surface, the current density is calculated using equation (2.58). The corona current is obtained by integrating the current density over the periphery of the coronating conductor(s). Multiplying the corona current by the applied voltage determines the corona power loss.

The calculated corona current agreed with those measured for monopolar (Abdel-Salam and Al-Hamouz, 1993, 1994, 1995b; Abdel-Salam et al., 1997; Al-Hamouz and Abdel-Salam, 1999) and bipolar lines (Abdel-Salam and Al-Hamouz, 1995a; Al-Hamouz et al., 1999).

5.5 CORONA NOISE

Corona noise includes interference with radio, television, and other wireless reception, caused by corona. Also, audible noise is experienced near EHV lines and substations. Corona undoubtedly interferes also with carrier signals transmitted along EHV lines.

The main source of corona radio noise is from positive streamers (Fig. 5.2), as their amplitudes are much higher than those of the negative Trichel pulses. As the pulses are random in amplitude, duration, and repetition rate, their noise is felt over a continuous spectrum. The noise level decreases at higher frequencies; this has been shown by both measurement and computation.

In measurements of the radio noise level and its lateral profile near bipolar HV DC lines, the highest level was recorded under the positive conductor whereas the noise contributed by the negative conductor was rather insignificant. For AC transmission lines, the lateral decay of radio noise is less steep than for DC lines.

In the case of AC corona, positive streamer pulses occur during the positive half-cycles and are also the main source of noise. At voltages slightly above the onset level, positive corona tends to take the form of a steady glow, assisted by the negative ions produced during the preceding negative half-cycles. Therefore, HV DC lines are usually more noisy than AC lines at voltage gradients slightly above the onset levels, particularly in fair weather.

5.5.1 Effect of Line Conductor Size

Radio interference (RI) measurements under both AC and DC EHV lines have shown that the RI level rises with the voltage gradient (i.e., field strength E_{max} at the HV conductor surface) according to the relation

$$\text{RI} = C(E_{max})^n \text{ dB} \tag{5.10}$$

C being a constant. For DC lines, the exponent n has a value of 5 to 7 in fair weather and 1.5 to 3.5 in rain. For AC lines, on the other hand, the exponent n is about 7 to 8 in both fair and foul weather.

For the same conductor voltage gradient, in both AC and DC lines, the RI level was found to increase with the conductor radius according to the relation

$$\text{RI} = C_1 r^2 \text{ dB} \tag{5.11}$$

This relation was found to be independent of conductor bundling.

5.6 SOLVED EXAMPLES

(1) Two parallel plates are spaced a distance d and are placed in SF_6 gas. One of the plates is stressed with a voltage V with respect to the other plate which is grounded. What would be the number of electrons in the avalanche growing between the plates? Neglect the effect of self-space charge of the avalanche on its growth.

Solution:
According to equations (3.41) and (3.44),

$$(\alpha - \eta)/p = A(E/p) + C, \qquad E = V/d$$

where

$A = 0.027$ and $C = -2400.4$

$$(\alpha - \eta) = AE + Cp \tag{5.12}$$

$$\begin{aligned} \text{Avalanche size} &= \exp[(\alpha - \eta)d] \\ &= \exp[AV + Cpd] \end{aligned} \tag{5.13}$$

(2) In problem (1), consider $d = 1\,\text{mm}$ and the gas pressure $p = 1\,\text{atm}$. Calculate the breakdown voltage V_s
(a) according to equation (4.13),
(b) corresponding to an avalanche size of 10^8,
(c) according to the criteria expressed by equations (5.4) and (5.5).

Solution:
(a) As γ is much smaller than unity, equation (4.13) is reduced to $\alpha = \eta$. According to equations (3.41) and (3.44), $\alpha = \eta$ occurs when

$$0.027(E/p) = 2400.4 \tag{5.14}$$

where

$E = V_s/d$

As $p = 101.3$ kPa,

$\therefore V_s = 9005.9\,\text{V} = 9\,\text{kV}$

(b) $p = 101.3$ kPa. According to equation (5.13)

$10^8 = \exp[AV + Cpd]$

where

$Cp = -2400.4 \times 101.3 = -24.32 \times 10^4$

$18.42 = 0.027V_s - 24.32 \times 10^4 \times 10^{-3}$

$V_s = 9689.6\,\text{V} = 9.70\,\text{kV}$

(c) As the avalanche self-space charge is neglected, the breakdown voltage will be the same irrespective of the polarity of the stressed plate.

According to the criteria expressed by equations (5.4) and (5.5)

$V_{s+} = 9.4\,\text{kV}, \qquad V_{s-} = 9.2\,\text{kV}$

(3) Repeat problem (2) for gas pressures of 3 and 5 atmospheres and comment on the results obtained.

Solution:
(a) According to equation (5.14),

$$V_s = 2400.4\,pd/0.027$$
$$= 2400.4 \times 3 \times 101.3 \times 10^{-3}/0.027\,\text{V}$$
$$= 27\,\text{kV at } p = 3\,\text{atm}$$

$$V_s = 2400.4 \times 5 \times 101.3 \times 10^{-3}/0.027\,\text{V}$$
$$= 45.03\,\text{kV at } p = 5\,\text{atm}$$

(b) According to equation (5.13),

$$10^8 = \exp[AV + Cpd]$$

$$18.42 = 0.027V_s - 24{,}004 \times 3 \times 101.3 \times 10^{-3}$$
$$V_s = 27.7\,\text{kV at } p = 3\,\text{atm}$$

$$18.42 = 0.027V_s - 24{,}004 \times 5 \times 101.3 \times 10^{-3}$$
$$V_s = 45.71\,\text{kV at } p = 5\,\text{atm}$$

(c) According to the criteria expressed by equations (5.4) and (5.5),

$$V_{s+} = 27.5\,\text{kV}, \qquad V_{s-} = 27.73\,\text{kV at } p = 3\,\text{atm}$$
$$V_{s+} = 45.2\,\text{kV}, \qquad V_{s-} = 45.5\,\text{kV at } p = 5\,\text{atm}$$

It is quite clear that the increase of gas pressure improves the dielectric strength of the gas since the breakdown voltage increases with gas pressure.

(4) Two concentric spheres have radii a and b, $b > a$. The interelectrode spacing is filled with SF_6 gas. The inner sphere is stressed with a voltage V with respect to the outer sphere, which is grounded. Determine the thickness of the ionization zone surrounding the inner sphere and the maximum size of the avalanche growing in this zone. Neglect the effect of self-space charge of the avalanche on its growth.

Solution:
At the ionization zone boundary $\alpha - \eta = 0$ where $E = E_i$. According to equation (5.12), $E_i = -Cp/A$ when $\alpha - \eta = 0$. With reference to Table 2.1,

$$E = \frac{V_{ab}}{r^2(b-a)} \tag{5.15}$$

$$-Cp/A = \frac{V_{ab}}{r_i^2(b-a)}$$

where r_i is the radius defining the ionization zone boundary.

$$r_i = \sqrt{\frac{V_{ab}A}{(b-a)Cp}} \tag{5.16}$$

Substituting E from equation (5.15) into equation (5.12),

$$\alpha - \eta = \frac{AV_{ab}}{r^2(b-a)} + Cp$$

The maximum avalanche size occurs when the avalanche grows over the whole thickness of the ionization zone.

$$\begin{aligned}\text{Maximum avalanche size} &= \exp\left[\int_a^{r_i}(\alpha-\eta)\mathrm{d}r\right] \\ &= \exp\left[\int_a^{r_i}\left(\frac{AV_{ab}}{r^2(b-a)}+Cp\right)\mathrm{d}r\right] \\ &= \exp\left\{\frac{AV_{ab}}{(b-a)}\left[\frac{1}{a}-\frac{1}{r_i}\right]+Cp(r_i-a)\right\}\end{aligned} \tag{5.17}$$

(5) In problem (4), consider $a = 0.1$ cm and $b = 2.1$ cm and the gas pressure $p = 1$ atm. Calculate the corona onset voltage

(a) corresponding to avalanche size of 10^8,
(b) according to the criteria expressed in equations (5.4) and (5.5).

Solution:

(a) Avalanche size is expressed by equation (5.17) which depends on the applied voltage V and the corresponding thickness r_i of the ionization zone; the latter depends also on V, as expressed by equation (5.16).

In equation (5.12) relating to $(\alpha - \eta)$,

$A = 0.027, \qquad C = -2400.4$

Given $a = 0.1 \times 10^{-2}$ m, $b = 2.1 \times 10^{-2}$ m, $p = 101.3$ kPa, solve equations (5.16) and (5.17) iteratively to get V_0 (corresponding to an avalanche size of 10^8) = 13.92 kV.

(b) According to the criteria expressed in equations (5.4) and (5.5),

$V_{0+} = 13.1\,\text{kV}$ and $V_{0-} = 13.7\,\text{kV}$

(6) Repeat problem (5) for gas pressures of 3 and 5 atmospheres and comment on the results obtained.

Solution:

(a) For $p = 3 \times 101.3\,\text{kPa}$, solve equations (5.16) and (5.17) iteratively to get V_0 (corresponding to an avalanche size of 10^8) = 34.6 kV.
For $p = 5 \times 101.3\,\text{kPa}$, solve equations (5.16) and (5.17) iteratively to get $V_0 = 54\,\text{kV}$.

(b) According to the criteria in equations (5.4) and (5.5),

$$V_{0+} = 34.9\,\text{kV}, \qquad V_{0-} = 35.1\,\text{kV at } p = 3\,\text{atm}$$
$$V_{0+} = 53.8\,\text{kV}, \qquad V_{0-} = 54.5\,\text{kV at } p = 5\,\text{atm}$$

It is quite clear that the increase of gas pressure results in increasing the corona onset voltage.

(7) Different flat arrangements of a three-phase transmission line are shown in Fig. 5.13. Each phase of the line has

(a) single conductor, Fig. 5.13a;
(b) bundle-2 conductor comprising two subconductors arranged in horizontal or vertical configuration, Fig. 5.13b;
(c) bundle-3 conductor with the three subconductors placed at the vertices of an upright or inverted triangle, Fig. 5.13c;
(d) bundle-4 conductor with the four subconductors placed at the vertices of a square, Fig. 5.13d;
(e) bundle-4 conductor with the four subconductors placed at the vertices of a diamond-form square, Fig. 5.13e.

Conductor radius = r, subconductor-to-subconductor spacing = s, phase-to-phase spacing = D, phase voltage = V. Calculate the corona onset voltage.

Solution:

It is evident that the surface field strength is higher at the middle phase than at the outer phases. The difference is normally about 7% for practical line dimensions.

The maximum field E_m values at the subconductor surface of the middle-phase of the line arrangements of Fig. 5.13 have already been expressed (Jha, 1977), where the effect of ground is disregarded (conductor height above ground $\gg$ phase-to-phase spacing D). The corona onset voltage is determined by the onset field E_0.

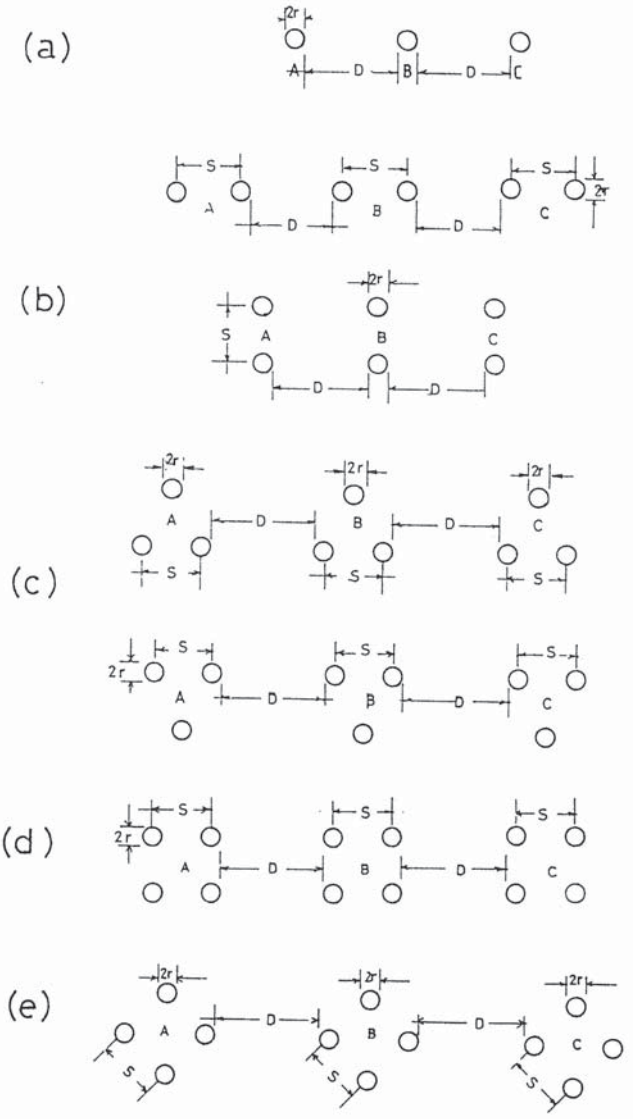

Figure 5.13 Three-phase transmission-line arrangements: (a) using single conductor; (b) using bundle-2 conductor arranged horizontally or vertically; (c) using bundle-3 conductor arranged at vertices of an upright or inverted triangle; (d) using bundle-4 conductor arranged at vertices of a square; (e) using bundle-4 conductor arranged at vertices of a diamond-form square.

(a) $$E_m = \frac{V}{r\ln(D/r)}$$

$$\therefore \text{Corona onset voltage } V_0 = E_0 r \ln(D/r) \tag{5.18a}$$

(b) $$E_m = \frac{V\left(1+\frac{2r}{s}\right)}{2r\ln\frac{D}{\sqrt{sr}}}$$

$$\therefore \text{Corona onset voltage } V_0 = 2E_0 r \ln\frac{D}{\sqrt{sr}} \Big/ \left(1+\frac{2r}{s}\right) \tag{5.18b}$$

(c) $$E_m = \frac{V\left(1+\frac{3\sqrt{3}r}{s}\right)}{3r\ln\frac{D}{\sqrt[3]{rs^2}}}$$

$$\therefore \text{Corona onset voltage } V_0 = 3E_0 r \ln\frac{D}{\sqrt[3]{\sqrt{2}rs^2}} \Big/ \left(1+\frac{3\sqrt{3}r}{s}\right) \tag{5.18c}$$

(d) $$E_m = \frac{V\left(1+\frac{4\sqrt{3}r}{s}\right)}{3r\ln\frac{D}{\sqrt[4]{\sqrt{2}rs^3}}}$$

$$\therefore \text{Corona onset voltage } V_0 = 4E_0 r \ln\frac{D}{\sqrt[4]{\sqrt{2}rs^3}} \Big/ \left(1+\frac{4\sqrt{2}r}{s}\right) \tag{5.18d}$$

(e) $$E_m = \frac{V\left(1+\frac{3\sqrt{2}r}{s}\right)}{4r\ln\frac{D}{\sqrt[4]{\sqrt{2}rs^3}}}$$

$$\therefore \text{Corona onset voltage } V_0 = 4E_0 r \ln\frac{D}{\sqrt[4]{\sqrt{2}rs^3}} \Big/ \left(1+\frac{3\sqrt{2}r}{s}\right) \tag{5.18e}$$

(8) For the arrangements of problem (7), calculate the positive and negative corona onset voltages at natural temperature and pressure if the subconductor radius $r = 1$ cm, subconductor-to-subconductor spacing $s = 40$ cm, and phase-to-phase spacing $D = 5$ m. Use the empirical formula reported in Section 5.3.

Solution:
According to the empirical formula

$$E_0 = 30\delta(1 + 0.3/\sqrt{\delta r})\,\text{kV}_{\text{peak}}/\text{cm}$$

where r is the conductor radius in cm.
At standard temperature and pressure, $\delta = 1$.

$$E_{0+} = 39\,\text{kV}_{\text{peak}}/\text{cm}$$

Using equations (5.18), the positive and negative corona onset voltages are calculated as:

(a) $V_0 = 6.2 \times 39 = 241.8\,\text{kV}_{\text{peak}}$
$= 171\,\text{kV}$

(b) $V_0 = 8.32 \times 39 = 342.48\,\text{kV}_{\text{peak}}$
$= 242.2\,\text{kV}$

(c) $V_0 = 9.97 \times 39 = 388.83\,\text{kV}_{\text{peak}}$
$= 274.9\,\text{kV}$

(d) $V_0 = 11.79 \times 39 = 459.81\,\text{kV}_{\text{peak}}$
$= 325.1\,\text{kV}$

(e) $V_0 = 12.16 \times 39 = 474.24\,\text{kV}_{\text{peak}}$
$= 335.3\,\text{kV}$

It is quite clear that the onset voltage increases with the increase of the number of subconductors per bundle.

(9) The conductors of a three-phase transmission line are placed at the vertices of an upright triangle of sides 5 m, 5 m, and 8.66 m.The radius of conductors $r = 1$ cm. Calculate the corona onset voltage at standard temperature and pressure.

Solution:
According to equation (5.18a)

$$V_0 = E_0 r \ln(D_{eq}/r)$$

D_{eq} = mean geometric distance between the conductors

$$= \sqrt[3]{5 \times 5 \times 8.66} = 6\,\text{m}$$

The corona onset field $E_0 = 30\delta(1 + 0.3/\sqrt{\delta r})$
At $\delta = 1$ at standard temperature and pressure,

$$E_0 = 39\,\text{kV}_{peak}/\text{cm}$$

$$V_0 = 39 \ln 600 = 249.5\,\text{kV}_{peak}$$
$$= 176.4\,\text{kV}(= 305.5\,\text{kV line-to-line})$$

(10) For the three-phase transmission line of problem (9), calculate corona power loss and the corona current when the line is operating at 50 Hz, 275 kV. Assume smoothness m_1 and weather m_2 coefficients are equal to 0.92 and 0.95, respectively. Atmospheric pressure and temperature are respectively equal to 75 cm Hg and 35° C.

Solution:

$$\text{Relative air density } \delta = \frac{3.92p}{273 + t}$$

where t is the temperature in °C and p is the pressure in cm Hg.

$$\delta = \frac{3.92 \times 75}{273 + 35} = 0.95$$

$$\text{The corona onset field } E_0 = 30\delta(1 + 0.3/\sqrt{\delta r})m_1 m_2$$
$$= 30 \times 0.95(1 + 0.3/\sqrt{0.95})0.92 \times 0.95$$
$$= 32.58\,\text{kV}_{peak}/\text{cm}$$

$$V_0 = 32.58 \ln 600 = 208.4\,\text{kV}_{peak}$$
$$= 147.37\,\text{kV}(255.25\,\text{kV line-to-line})$$

$$V_0 = 275/255.25 = 1.078$$

The corresponding value of the K factor (Fig. 5.10) = 0.05. According to Peterson's formula (5.6),

$$\text{Corona power loss } P_c = \frac{3.73 \times 0.05}{(D_{eq}/r)^2} f V_{ph}^2 \times 10^{-5} \text{ kW/(cond.km)}$$

$$= \frac{3.73 \times 0.05 \times 50 \times (275 \times 10^3/\sqrt{3})^2}{(600)^2} \times 10^{-5}$$

$$= 6.53 \text{ kW/(cond.km)} = 19.6 \text{ kW/km}$$

$$\text{Corona current } = P_c/V_{ph} = 6.53 \times 10^3/(275 \times 10^3/\sqrt{3}) \text{ A}$$

$$= 41.1 \text{ mA/km}$$

(11) A single conductor, 3.175 cm radius, of a 525 kV line is strung 13 m above ground. Calculate (a) the corona onset voltage and (b) the effective radius of the corona envelope, at a voltage of 2.5 p.u. (i.e., 2.5 times rated voltage). Consider smoothness m_1 and weather m_2 factors are both equal to 0.9. Relative air-density factor = 1.

Solution:

(a) $E_0 = 30\delta(1 + 0.3/\sqrt{\delta r})m_1 m_2 = 30(1 + 0.3/\sqrt{3.178})0.9 \times 0.9$

$$= 28.4 \text{ kV}_{peak}/\text{cm}$$

$$= 20 \text{ kV/cm}$$

$$V_0 = E_0 r \ln(2h/r) = 426 \text{ kV}$$

$$= 426\sqrt{3} = 737.8 \text{ kV (line-to-line)}$$

At 525 kV line-to-line operating voltage, there is no corona present.

(b) 2.5 p.u. voltage = $2.5 \times 525 = 1312.5$ kV (line-to-line), which is higher than the onset voltage, so corona is present on the conductor. The corona envelope around the conductor is considered an extension to its radius.

When considering the effective radius of the corona envelope r_e, one may assume a smooth surface of the envelope.

$$1312.5\sqrt{2}/\sqrt{3} \text{ kV}_{\text{peak per phase}} = E_0 r_e \ln(2H/r_e)$$

$$= 30(1 + 0.3/\sqrt{r_e})r_e \ln(2600/r_e)$$

where r_e is the envelope radius in cm.

A trial and error solution yields $r_e = 5$ cm. This represents an increase in conductor radius r by about 57%.